Journal of Magnetic Resonance 328 (2021) 106981

Contents lists available at ScienceDirect

Journal of Magnetic Resonance

journal homepage: www.elsevier.com/locate/jmr

Molecular self-diffusion in internal magnetic fields of porous medium investigated by NMR MGSE method ☆

Janez Stepišnik [a,*], Ioan Ardelean [b], Aleš Mohorič [a]

[a] University of Ljubljana, Faculty of Mathematics and Physics, Physics Department, Jadranska 19, 1000 Ljubljana, Slovenia
[b] Physics Department, Faculty of Materials Science and Engineering, Technical University of Cluj-Napoca, Romania

ARTICLE INFO

Article history:
Received 13 February 2021
Revised 8 April 2021
Accepted 9 April 2021
Available online 20 April 2021

Keywords:
NMR spin echo
Porous media
Self-diffusion measurement
Magnetic susceptibility
Very in-homogeneous magnetic field
Molecular velocity auto-correlation
Magnetic impurities

ABSTRACT

Inhomogeneous magnetic fields generated in porous media due to differences in magnetic susceptibility at solid/liquid interfaces and due to intrinsic or artificially doped magnetic impurities can be used to gain insight into the molecular dynamics of fluid in the structure of a porous medium using the concept of NMR modulated gradient spin echo method. We extended the theory of this method to the case of an inhomogeneous magnetic field that cannot be approximated by an uniform gradient, in order to explain the CPMG measurements of self-diffusion in water soaked ceramics, which are doped with magnetic impurities of different contents. The new interpretation provides the spin relaxation times, the average pore size and their distribution, as well as the strength of the internal magnetic gradient fields in the doped ceramics.

1. Introduction

Porous materials are relevant in biology and technology. Such materials have been extensively studied by NMR methods. Together with relaxation at pore walls additional attenuation of NMR signal because of diffusion in internal gradients can be observed. In many cases, diffusion of the spins in the fluid phase through these internal inhomogeneities controls the transverse decay rate of the NMR signal. In measuring molecular motion a highly heterogeneous liquid-soaked porous material [1] by the NMR gradient spin-echo (GSE) method artifacts can appear either due to deficiencies in the homogeneity of the externally applied magnetic field or due to internal fields induced by the susceptibility differences between the solid matrix and liquid, when samples are introduced in an external magnetic field. The strength of internally induced inhomogeneous magnetic fields (IMFs), which can be further enhanced by the presence of magnetic impurities, overlaps the externally applied IMF with a homogeneous magnetic field gradient $\vec{G} = \nabla\left|\vec{B}_{eg}\right|$ (MFG). Thus, a detailed evaluation of the experimental data that contains information of the pore structure is quite difficult. Several methods of measuring relaxation and diffusion in porous media have been developed and they can provide information on pores sizes, their distribution and on internal gradients [2–8]. However, the internal magnetic fields limit the use of GSE measurements to samples with low internal IMF [9] and also reduce the resolution of magnetic resonance images [10,11]. There are techniques to overcome this problem using compensating gradient pulse sequences [12].

Research has shown that the internal IMF may have not only a negative role, but can serve as a tool to exploit the structure of porous media by using the concept of the modulated gradient spin-echo method (MGSE) [13]. The MGSE method allows insight into molecular motion by measuring directly the velocity autocorrelation function of the spin bearing particles. This quantity contains detailed information about the molecular translation dynamics. In the MGSE method the spatial dispersion of spin phase is modulated by a sequence of radio-frequency pulses (RF) and pulses or waveform of MFG. The role of the MFG can be taken over by IMF of the porous media [14]. The method is able to measure not only the self-diffusion coefficient but also provides an insight into the low-frequency part of the velocity auto-correlation spectrum. In the introduction of this paper, we will develop a theoretical formalism of spin dynamics under the influence of a sequence RF

☆ This document is the results of the research project funded by the Slovenian research agency, ARRS, under the program P1-0060, "Experimental biophysics of complex systems and imaging in bio-medicine" and the grant PN-III-P4-ID-PCE-2020-0533 from the Romanian National Authority for Scientific Research.

* Corresponding author.
E-mail address: janez.stepisnik@fmf.uni-lj.si (J. Stepišnik).
URL: http://www.fmf.uni-lj.si/stepisnik/index.html (J. Stepišnik).

https://doi.org/10.1016/j.jmr.2021.106981
1090-7807/

pulses and such IMF, which does not allow the usual MFG approximation. The derived formulas for spin-echo attenuation are compared with experimental data on the diffusion of water in ceramics doped with magnetic impurities at the end.

2. NMR gradient spin echo in highly inhomogeneous magnetic field

Using an NMR GSE method to study the molecular translation dynamics of liquid confined in the structure of porous medium, we assume that the rapid molecular motion on the time scale of pico- or nanoseconds completely nullifies the spin dipole-dipole and the first order quadrupole interactions. We will consider the case, where the RF and applied magnetic field **B** are strong enough that the signal attenuation due to the spin velocity fluctuation in IMF prevails over the spin interactions with electrons in molecular orbitals and the electron mediated spin-spin interactions. Thus, their influence is reflected in only in fluctuations of relevant physical quantities, affecting the spin relaxation of spin bearing particles at least in the first approximation.

We assume that the spins interact with the magnetic field, which consists of the main uniform static magnetic field B_{0z}, radiofrequency (RF) field and IMF. B_{0z} is applied externally along the z-axis and is associated with the spin Larmor precession frequency ω_0. IMF $\mathbf{B}_{in}(\mathbf{r})$ can be applied externally or is inherent to the sample and causes a deviation ω_{in} from the Larmor frequency. The RF magnetic pulses $B_{rf}(t) = \omega_{rf}(t)/\gamma$ start with $\pi/2$ pulse with the field aligned along the x-axis to excite spins in a narrow spatial area of the sample, which is followed by a single or a sequence of π-RF pulses aligned along the y-axis. If $\omega_0 \gg |\omega_{in}|$ all the concomitant components of IMF can be neglected. Given that the treatment of the spin dynamics governed by the time-varying magnetic fields and the RF pulses is not simple, we will limit our consideration to a static IMF, where we must consider that in the interval of simultaneous action of the static magnetic field and the RF pulses the resonant offset causes the signal undulation [15]. However, this effects can be ignored, as the spin excitation range created by the initial $\pi/2$-RF pulse applied in the fixed IMF is narrow enough that the signal undulation is reduced to less than 1% of the signal amplitude. Thus, the y-component of magnetization induces the spin echo signal at time t that can be approximated by [16]

$$E(t) \propto \sum_j \left\langle \mathrm{e}^{i\int_0^t \omega_{in}(\mathbf{r}_j(t'))\cos(b(t'))dt'} \right\rangle, \tag{1}$$

where j denotes the spin at $\mathbf{r}_j$, and where $b(t) = \int_0^t \omega_{rf}(t')dt'$ describes the effect of the sequence of π-RF pulses that flips spins around y-axis (or effectively changes the sign of ω_{in}) after each π-RF pulse). At the peak of spin echo $t = NT$, where T is the interval between two consecutive π-RF-pulses, the signal refocuses with $f_\pi(NT) = \int_0^{NT} \cos(b(t))dt = 0$, which allows the integration per-parts to get the amplitude of the peak of the N-th echo as

$$\begin{aligned} E(NT) \propto & \sum_j \left\langle \mathrm{e}^{-i\int_0^{NT} \dot{\omega}_{in}(\mathbf{r}_j(t))f_\pi(t)dt} \right\rangle = \\ = & \sum_j \left\langle \mathrm{e}^{-i\int_0^{NT} \nabla\omega_{in}(\mathbf{r}_j(t))\cdot\mathbf{v}_j(t)f_\pi(t)dt} \right\rangle. \end{aligned} \tag{2}$$

Particle velocity, $\mathbf{v}_j$, is encoded in the amplitude of the spin-echo, which indicates that the GSE methods allow not only to measure the self-diffusion coefficient, but it also offers the acquisition of more detailed information on the molecular translation dynamics.

When taking into account the stochastic nature of molecular self-diffusion, the measurement with the PGSE method in short gradient pulse limit, Eq. (2) appears in the form of a characteristic functional of the stochastic process, which is a Fourier transform of the probability distribution of spin bearing particles [17]. It was used by Stejskal [18] to show that instead of the Bloch-Torey equations [19] with which we cannot analyze the GSE decay of restricted self-diffusion, the methodology of the GSE as the Fourier transform of the particle probability distribution can be used. This approach provides a clear analogy with a tracer spreading in the medium that leads to the averaged propagator approach [20] from which the concept of diffusive diffraction of spin echo in a porous media has been developed [21], where the important requirement must be met that the gradient pulses are shorter than the characteristic times of molecular diffusion. However, the methodology of statistical physics can be used quite generally by expanding Eq. (2) as a characteristic functional of the probability distribution in a series of cumulants with respect to randomly fluctuating spin phase discord $\nabla\omega_{in}(\mathbf{r}_j(t))$ [22] created by any MFG sequence of finite width pulses or waveform.

Assuming that the molecular displacements in the interval T are shorter than the grating of the spatial spin phase discord created by the RF/IMF sequence,

$$\sqrt{2DT} < \frac{2\pi}{\gamma|\mathbf{G}|T},$$

which is a motional averaging regime according to Hürlliman's [23,24], the decay of the echo amplitudes in Eq. (2) can be approximated by the cumulant series to the second order [25]

$$E(\tau) \approx \sum_j \mathrm{e}^{i\phi_j(\tau)-\beta_j(\tau)+\cdots}, \tag{4}$$

which is the Gaussian phase approximation (GPA) [26–28]. Here, the signal phase shift is related to the mean of the fluctuation of the spin phase change rate (SPCR), $\dot{\omega}_{in}(\mathbf{r}_j(t)$

$$\phi_j(\tau) = -\int_0^\tau \langle \dot{\omega}_{in}(\mathbf{r}_j(t))\rangle f_\pi(t)dt, \tag{5}$$

in which $\langle \dot{\omega}_{in}(\mathbf{r}_j(t))\rangle = \nabla\omega_{in}(\mathbf{r}_j(t)) \cdot \langle \mathbf{v}_j(t)\rangle$ with $\nabla\omega_{in}(\mathbf{r}_j(t))$ being the gradient of internal IMF multiplied with gyro-magnetic ratio γ. The phase shift can be neglected if the mean spin velocity is equal to zero, $\langle \mathbf{v}_j(t)\rangle = 0$, such as when there are no flows in the fluid. However, this is not the case for the diffusion in inhomogeneous medium, where locally non-zero means of spin displacements cause effects such as "diffusion diffraction", the signal decay feature in porous medium that was first derived from the average propagator approach [21] and later explained by the phase shift of the signal [28].

The signal attenuation in Eq. (4) can be expressed as

$$\beta_j(\tau) = \int_0^\tau \int_0^t C_v(\mathbf{r}_j(t), \mathbf{r}_j(t'))f_\pi(t')f_\pi(t)dt'dt \tag{6}$$

where the auto-covariance of SPCR

$$\begin{aligned} C_v(\mathbf{r}_j(t), \mathbf{r}_j(t')) = & \langle \dot{\omega}_{in}(\mathbf{r}_j(t'))\dot{\omega}_{in}(\mathbf{r}_j(t))\rangle - \langle \dot{\omega}_{in}(\mathbf{r}_j(t'))\rangle \\ & \times \langle \dot{\omega}_{in}(\mathbf{r}_j(t))\rangle, \end{aligned} \tag{7}$$

is equal to the difference between the auto-correlation function of SPCR and the product of the mean SPCR at different times. By using the Wiener-Khinchin theorem [29,30], this equation can be converted from the time domain to the frequency domain by inserting a Fourier transform

$$C_v(\mathbf{r}_j(t), \mathbf{r}_j(0)) = \frac{1}{\pi}\int_{-\infty}^{\infty} C_v(\omega, \mathbf{r}_j)\,\mathrm{e}^{i\omega t}d\omega \tag{8}$$

to obtain

$$\beta_j(\tau) = \frac{1}{\pi}\int_0^\infty C_v(\omega,\mathbf{r}_j)|f_\pi(\omega)|^2 d\omega \tag{9}$$

where $f_\pi(\omega)$ is the modulation spectrum of the spin phase discord. Following the fact that the second time derivative of the mean square displacement is proportional to the velocity correlation function of the particle, the same can be used to obtain the spectrum $C_v(\omega,\mathbf{r}_j) = XX(\omega,\mathbf{r}_j) - X^2(\omega,\mathbf{r}_j)$. It consists of the difference between the Fourier cosines transform (FCT) of the mean squared difference of $\omega_{in}(\mathbf{r}_j(t))$

$$XX(\omega,\mathbf{r}_j) = -\frac{\omega^2}{2}FCT\left(\left\langle(\omega_{in}(\mathbf{r}_j(t)) - \omega_{in}(\mathbf{r}_j(0)))^2\right\rangle\right) \tag{10}$$

and FCT of the square of $\omega_{in}(\mathbf{r}_j(t))$ mean difference

$$X^2(\omega,\mathbf{r}_j) = -\frac{\omega^2}{2}FCT\left(\left\langle(\omega_{in}(\mathbf{r}_j(t)) - \omega_{in}(\mathbf{r}_j(0)))\right\rangle^2\right) \tag{11}$$

In cases of turbulence in the fluid flow, the auto-covariance is equal to the auto-correlation of the stochastic components of the velocity $\left\langle \mathbf{v}_j'(t)\mathbf{v}_j'(t')\right\rangle$, which $\mathbf{v}_j'$ is fluctuating component of the molecular velocity $\mathbf{v}_j(t)$ caused by random motions. It is similar in the case of the self-diffusion in an unbounded liquid without any flow components, $\langle \mathbf{v}_j(t)\rangle = 0$, where the homogeneous gradient $\dot{\omega}_{in}(\mathbf{r}_j(t)) = \gamma\mathbf{G}(t)\mathbf{v}_j(t)$ with $\mathbf{G}(t) = \nabla B_{zin}(t)$ gives the spin echo attenuation

$$\beta_j(\tau) = \frac{1}{\pi}\int_0^\infty \mathbf{q}(\omega,\tau)\underline{D}_j(\omega,\tau)\mathbf{q}^*(\omega,\tau)\,d\omega, \tag{12}$$

where $\mathbf{q}(\omega,\tau)$ denotes the spectrum of the spin phase discord $\mathbf{q}(t) = \gamma\int_0^t \mathbf{G}(t')f_\pi(t')dt'$, and $\boldsymbol{D}_j(\omega,\tau)$ is the tensor of the velocity auto-correlation spectrum (VAS)

$$\mathbf{D}_j(\omega,\tau) = \int_0^\infty \langle \mathbf{v}_j(t)\otimes\mathbf{v}_j(0)\rangle_\tau \cos(\omega t)dt. \tag{13}$$

With the above consideration, we correct some erroneous procedure in the treatment of diffusion in a porous system, when the square of the mean particle displacement is not taken into account in the expression for signal attenuation. It is quite commonly forgotten that it is not necessary if the FT of a time-dependent function is equal to zero, that it is also the FT of the square of this time function. This fact was also ignored in our previous consideration of this subject [13].

2.1. Modulated gradient spin echo method

Among the NMR GSE methods for measuring the molecular diffusion the MGSE method [27] stands up, in which the CPMG RF sequence [31,32] is combined with MFG [26,33] in order to modulate the spatial distribution of the spin phase in a way to get a direct insight in the key quantity of molecular dynamics in liquids, i.e. the velocity autocorrelation spectrum (VAS). The sequence creates the spectrum of the spin phase discord $|f_\pi(\omega)|^2$ with a single dominant peak that allows to pick up the value of VAS at the modulation frequency $\omega_m = \pi/T$. The MGSE method with pulsed and sinusoidal gradient wave-forms has been used to study flow through porous media [33], restricted diffusion in porous media [14,34–36] and diffusion in emulsions [35,37,38]. Its upper sampling frequency is limited below 1 kHz at the present state of the art by the MFG pulse switching rate, which is determined by the inductance of the gradient coils. No such upper limit applies to the method that combines CPMG-RF pulses with the stationary MFG [39,40,13], as the switching rate is given by the inverse time interval between the RF pulses and thus enables much higher frequency limit, determined by the power of the RF transmitter and the magnitude of the MFG. This technique has been proposed for the first time in [27] together with a concern about the side effects introduced by the application of RF pulses in the background of IMF. It causes the resonance offset effect, which depends on the width of the excited spin range [40,13]. It was shown that if the region of exited spins is narrow enough, the resonance offset only slightly undulates the echoes peaks of MGSE measurements in a fixed IMF [15,28].

Considering the case, in which the fixed IMF is generated by the differences in magnetic susceptibility and/or magnetic impurities in porous matrix [13,1], the CPMG train of π-RF pulses creates the power spectrum of the spin phase discord in the form of a triangle wave

$$|f_\pi(\omega,N)|^2 = \frac{8\sin^4\left(\frac{\tau\omega}{4}\right)\sec^2\left(\frac{\tau\omega}{2}\right)\left(1+(-1)^{N+1}\cos(N\tau\omega)\right)}{\omega^4}, \tag{14}$$

which depends on the consecutive order N of the spin echo as shown in Fig. 1. Its form varies from a wide lobe of the first echo ($N = 1$), with area under the lobe $\pi T^3/12$ and maximum at zero frequency, to narrow peak with the maximum at the frequency $\omega_m = \pi/T$ and area $\frac{4NT}{\pi\omega_m^2}$ for the echoes with $N > 1$. The peaks increase and get narrower as N increases. Echoes also have spectral bulges at a higher frequency $\omega = 3\pi/T$, but their areas are by a factor $\frac{2}{81}$ smaller than that of the peaks at ω_m. Assuming that the spectrum of $C_v(\omega)$ or $\boldsymbol{D}(\omega)$ is almost constant in the frequency interval of the peak width, $1/NT$, we can approximate

$$|f_\pi(\omega,N)|^2 = \frac{4NT}{\pi\omega_m^2}\delta(\omega-\omega_m) + \ldots \tag{15}$$

to get the spin echo in the form

$$E(\omega_m,NT) \approx \sum_j \mathrm{e}^{-\frac{NT}{T_{2j}}-\frac{4NT}{\pi^2\omega_m^2}C_v(\omega,\mathbf{r}_j)_{NT}}, \tag{16}$$

in which also the spin relaxation T_2 is taken into account. By changing the intervals between π-RF pulses, the peak of $|f_\pi(\omega,N)|^2$ can be adjusted in position along the frequency domain in order to trace out the spectrum $\underline{C_v}(\omega,\mathbf{r}_j)_{NT}$. However, we need to keep in mind that the index NT in $\langle\ldots\rangle_{NT}$ means average over the elapsed particle trajectory during the interval NT, whereby both the extent of interaction of the spin-bearing particle with the internal field and with the structure of the porous structure are changing [13]. Initially, at short time intervals, the interactions are not yet completely averaged and spins at different starting points contribute signals with different decay rates, α, to the echo in Eq. (16). The decay rate distribution $P(\alpha)$ gives the signal $E(t) = \int P(\alpha)e^{-\alpha t}d\alpha$, which can be approximated in the case of a narrow distribution as [41]

$$\ln\left(\sum_j \mathrm{e}^{-\alpha_j t}\right) \approx c - \langle\alpha\rangle t + \frac{1}{2!}\langle\alpha^2\rangle t^2 - \frac{1}{3!}\langle\alpha^3\rangle t^3 + \ldots \tag{17}$$

Here $\langle\alpha\rangle$ is the mean decay, and $\langle\alpha^n\rangle$ is the n-th central moment of α distribution respectively. Thus, in the polynomial expansion of the logarithm of the non-exponential decay of the spin echo attenuation, the quadratic term gives the variance of the distribution, while the cubic term gives its skewness, which is a measure of the degree of asymmetry of the distribution. As $C_v(\omega,\mathbf{r}_j)_{NT}$ depends on the length of the spin trajectories across the pore space and through pore interconnections, the variance and skewness can vary according to the duration of the measurement interval. However, we must be aware that a non-exponential decay can also occur in cases of diffusion in a multi-component system, in an-isotropic diffusion and also in a porous medium due to the dispersion of pore sizes [42].

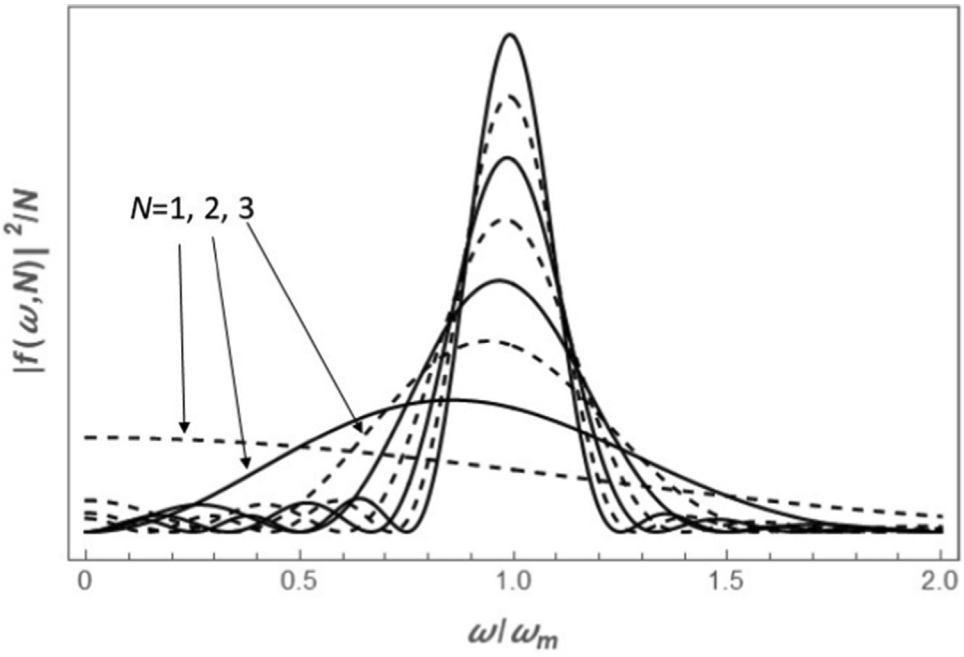

Fig. 1. The power spectra of the spin phase discord of the spin echoes with odd (dashed) and even (solid) sequential number *N*.

Table 1
Samples.

Sample	Fe_2O_3 %w/w	$\Delta\chi \times 10^5$ (sample-water)
S0	0	2.9
S2	2	4.9
S4	4	7.1
S6	6	8.7
S8	8	11.2

2.2. Diffusion in an internal field of porous media

In an inhomogeneous system like a porous medium the molecular Brownian motion can be treated in different ways. By solving either the Langevin equation [43] or the Fick diffusion equation with the boundary condition given by the solid matrix. The solution of the Fick's equation gives the probability density of a particle displacement from location $\mathbf{r}_0$ to $\mathbf{r}$ in the time t, for an arbitrary pore geometry

$$P(\mathbf{r}, t|\mathbf{r}_o) = \sum_{\mathbf{k}} \psi_{\mathbf{k}}(\mathbf{r})\psi_{\mathbf{k}}(\mathbf{r}_o)\, \mathrm{e}^{-t/\tau_{\mathbf{k}}}. \tag{18}$$

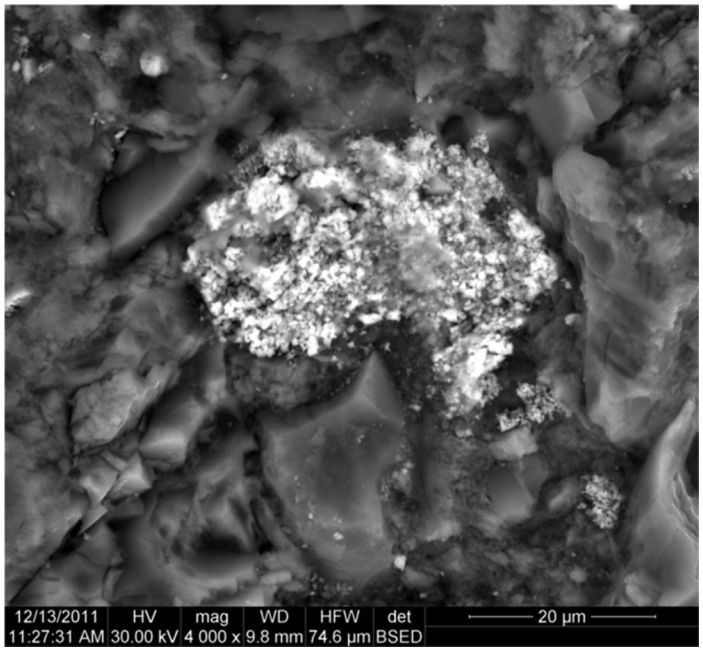

Fig. 2. SEM image of the sample S4.

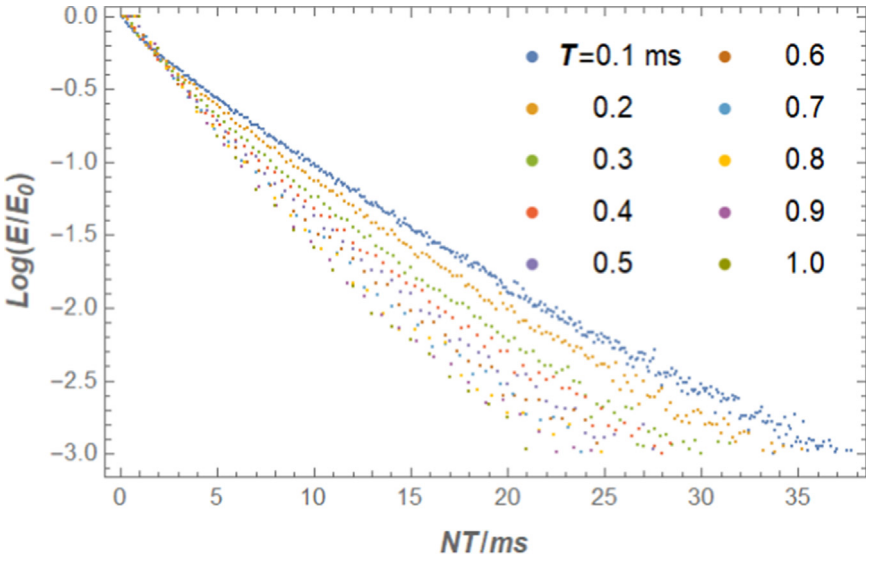

Fig. 3. Spin echoes decays for sample *S4* .

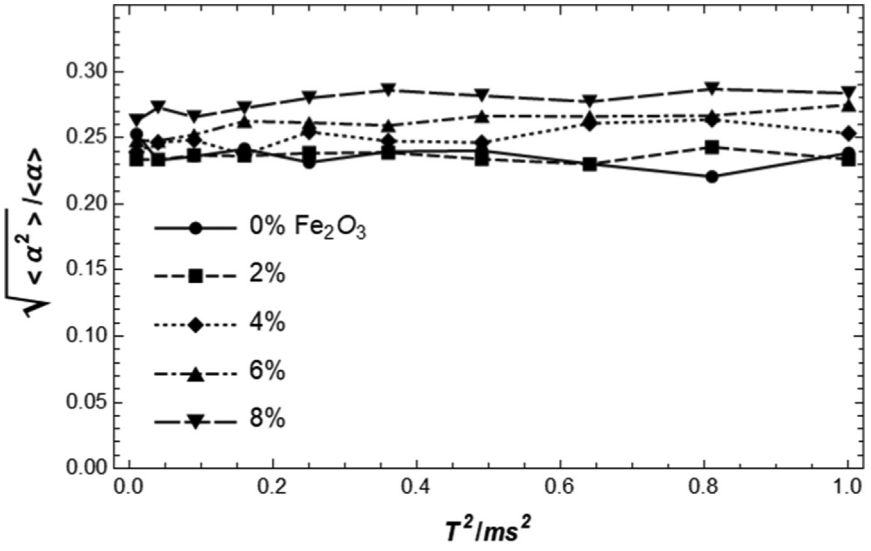

Fig. 4. The dependence of the relative variance of the decay time distribution $\sqrt{\langle\alpha^2\rangle}/\langle\alpha\rangle$ on the squared interval, T^2, between π-RF pulses at different contents of magnetic impurities.

Here $\tau_{\mathbf{k}}$ and $\psi_{\mathbf{k}}(\mathbf{r})$ are the characteristic times and the eigen functions of the **k**-th diffusion mode respectively. In a system where a strong IMF created by the susceptibility difference determines $\omega_{in}(\mathbf{r}_j(t))$, according to the Wiener-Khinchine theorem [29] the second derivative of the mean square displacement (MSD) is related to the correlation functions as follows [44,13]. Thus, we can express the mean squared difference

$$\left\langle \left(\omega_{in}(\mathbf{r}_j(t)) - \omega_{in}(\mathbf{r}_j(0))\right)^2 \right\rangle = \sum_{\mathbf{k}} \langle \Delta\omega_{\mathbf{k}}^2(\mathbf{r}_j)\rangle \psi_{\mathbf{k}}(\mathbf{r}_j)\, \mathrm{e}^{-t/\tau_{\mathbf{k}}} \tag{19}$$

and the mean difference

$$\left\langle \left(\omega_{in}(\mathbf{r}_j(t)) - \omega_{in}(\mathbf{r}_j(0))\right) \right\rangle = \sum_{\mathbf{k}} \langle \Delta\omega_{\mathbf{k}}(\mathbf{r}_j)\rangle \psi_{\mathbf{k}}(\mathbf{r}_j)\, \mathrm{e}^{-t/\tau_{\mathbf{k}}} \tag{20}$$

where $\langle \Delta\omega_{\mathbf{k}}^2(\mathbf{r}_j)\rangle$ and $\langle \Delta\omega_{\mathbf{k}}(\mathbf{r}_j)\rangle$ are calculated as

$$\langle \Delta\omega_{\mathbf{k}}^n(\mathbf{r})\rangle = \frac{1}{V}\int_V (\omega_{in}(\mathbf{r}) - \omega_{in}(\mathbf{r}_o))^n \psi_{\mathbf{k}}(\mathbf{r}_o) d\mathbf{r}_o \tag{21}$$

This gives the power spectrum [44]

$$C_v(\omega, \mathbf{r}_j) = C_{XX}(\omega, \mathbf{r}_j) - C_{X2}(\omega, \mathbf{r}_j). \tag{22}$$

where

$$C_{XX}(\omega, \mathbf{r}_j) = -\frac{1}{2}\sum_{\mathbf{k}} \langle \Delta\omega_{\mathbf{k}}^2(\mathbf{r}_j)\rangle \psi_{\mathbf{k}}(\mathbf{r}_j) \frac{\tau_{\mathbf{k}}\omega^2}{1+\tau_{\mathbf{k}}^2\omega^2} \tag{23}$$

is the FCT of the mean squared difference and the FCT of the squared mean difference is

$$C_{X2}(\omega, \mathbf{r}_j) = -\frac{1}{2}\sum_{\mathbf{k}}\sum_{\mathbf{n}} \langle \Delta\omega_{\mathbf{k}}(\mathbf{r}_j)\rangle \langle \Delta\omega_{\mathbf{n}}(\mathbf{r}_j)\rangle \psi_{\mathbf{k}}(\mathbf{r}_j)\psi_{\mathbf{n}}(\mathbf{r}_j) \times \frac{\omega^2\tau_{\mathbf{k}}\tau_{\mathbf{n}}(\tau_{\mathbf{k}}+\tau_{\mathbf{n}})}{(\tau_{\mathbf{k}}+\tau_{\mathbf{n}})^2 + \tau_{\mathbf{k}}^2\tau_{\mathbf{n}}^2\omega^2} \tag{24}$$

The molecular motion between the boundaries of porous structure and through internally generated IMF brings about a spin echo attenuation dependence on the spin location, $\mathbf{r}_j$ in Eq. (9). This is

shown in Fig. 5 for the cases of IMF with the homogeneous gradient, G, and for the case of the bell shaped susceptibility induced IMF [10]. The latter causes a large dispersion of damping within the pore, leading to non-exponential decay with the covariance $\langle\alpha^2\rangle$ having a strong time-dependence.

As we can see, the spin echo attenuation derived from Eqs. (17), (16), and (22)

$$\langle\alpha\rangle = \frac{1}{T_2} + \frac{4}{\pi^2\omega_m^2}\langle C_v(\omega_m)\rangle, \tag{25}$$

is generally determined by a set of characteristic times. However, if the intervals between π-RF pulses T are long enough to be comparable with the longest characteristic times, the magnitudes of which is about the time of flight of the particle over the pore volume, the following approximation can be used

$$\langle C_v(\omega_m)\rangle \approx \frac{\langle\Delta\omega_0^2\rangle}{\tau_0} + \left(\langle\Delta\omega_1^2\rangle - \langle\Delta\omega_{01}\rangle\right)\frac{\omega_m^2\tau_1}{1+\tau_1^2\omega_m^2} - \langle\Delta\omega_{11}\rangle \times \frac{\omega_m^2\tau_1/2}{1+\omega_m^2\tau_1^2/4} + \ldots. \tag{26}$$

Here $\langle\Delta\omega_{\mathbf{k}}^2\rangle = -\frac{1}{2V}\int_V\langle\Delta\omega_{\mathbf{k}}(\mathbf{r}^2)\rangle\psi_{\mathbf{k}}(\mathbf{r})d\mathbf{r}$ and $\langle\Delta\omega_{\mathbf{kn}}\rangle = -\frac{1}{2V}\int_V\langle\Delta\omega_{\mathbf{k}}(\mathbf{r})\rangle\langle\Delta\omega_{\mathbf{n}}(\mathbf{r})\rangle\psi_{\mathbf{k}}(\mathbf{r})\psi_{\mathbf{n}}(\mathbf{r})d\mathbf{r}$ and where τ_0 and τ_1 are the longest correlation times. Here the integration over the volume V includes pores together with their interconnections. The inter-pore diffusivity is described by the first term, which is commonly written as $D_p = \alpha_t D$ with a_t being the tortuosity factor. It is the ratio between the long-range and the local molecular self-diffusion D, and formally can be written as $a_t = \langle\Delta\omega_0^2\rangle/\tau_0 D$. Here τ_1 denotes the mean time of flight over pore volume, while τ_0 includes the time of the pore interconnection crossing.

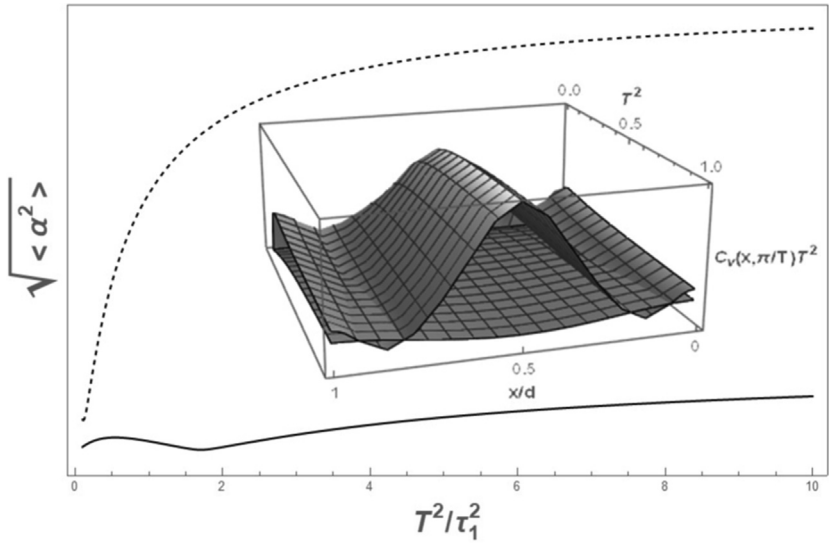

Fig. 5. The square root of variances of the non-exponential spin echo decay $\sqrt{\langle\alpha^2\rangle}$ for diffusion between the between plan-parallel pores for the cases of IMF with the homogeneous gradient (solid) and for the case of internally induced IMF (dashed). Both are calculated from the spatial dispersion of the power spectra $C_v(\omega, \mathbf{r})$ (inserted) for the examples of a homogeneous gradient (bottom) and an internally induced bell-shaped IMF (top).

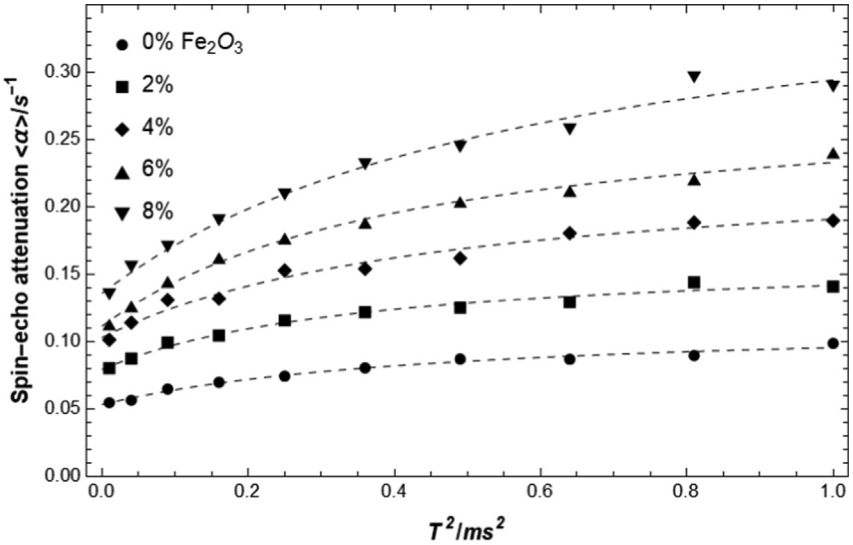

Fig. 6. The average decay rate of the spin-echos, $\langle\alpha\rangle$, as a function of T^2 at different concentrations of magnetic impurities (points) together with the fits to Eq. (26) (curves).

3. Experiment

Samples investigated in our experiment were prepared using the approach described in Ref. [45]. They were manufactured under identical conditions (ingredients, pressure, temperature) but contain an increased amount of magnetic impurities (iron oxide III). The iron oxide content of the samples is shown in Table 1 together with the susceptibility difference between the ceramic and water measured at 0.47 T with a vibrating magnetometer. Due to the identical preparation approach and the relatively small amount of magnetic impurities, we expect the same pore size. In the SEM image of the sample S4 shown in Fig. 2 a clustered structure of iron oxide is observed, and also the inter-granular spaces the size of about 2–3 micrometers.

The obtained samples were introduced in NMR tubes with 10 mm external diameter, which fit inside a low field NMR instrument (Bruker MINISPEC MQ20,3 Bruker, Germany) operating at 20 MHz proton resonance frequency. To avoid the edge effects on our measurements we used bigger amount of sample, exceeding the active volume of RF coil. The amplitude of spin-echoes, which are created by the CPMG train of π-RF pulses, were recorded by increasing inter pulse spacing between 0.1 and 1 ms, where the lower limit was set by the hardware limitations of our NMR instrument. We consider the CPMG sequence applied in the background of the internal IMF inside a porous medium as an MGSE sequence that enables to provide the spectrum of molecular motion of the liquid soaked ceramics. With the magnetic impurities artificially added to a porous ceramic we change the internal IMF already created inside the samples by other impurities and a susceptibility difference between a liquid and a solid, we can get a better insight into the role that the internal IMF play in the measuring of molecular self-diffusion in porous media.

4. Results and discussion

CPMG measurements of ceramics doped with different contents of magnetic impurities show a deviation from the monoexponential time decays of spin echoes at different intervals between RF pulses T, as shown in Fig. 3, where the signal E_0 is determined by extrapolating the first echoes to the initial time. In the logarithmic description of the signal decay, the deviated decay can be well fitted with a second-order polynomial, while an attempt to fit with a higher-order polynomial gives poorer results. The fits give the average decay rates and the variances of the decay rate distributions according to Eq. (17) for all samples. In heterogeneous system, such non-exponential decays are commonly attributed to the distribution of decay rate due to a pore size dispersion in porous medium [42], but this may also be due to the distribution of the internal IMF within the pore and perhaps even to the inhomogeniety of the VAS within the pore space as shown in Fig. 5. This figure shows the results of the exact calculation for the diffusion between the between plan-parallel pores in the case of IMF with the uniform gradient and in the case of internally induced bell-shaped IMF. The inserted figure shows the spatial dispersion of the power spectra $C_v(\omega, \mathbf{r})$ for both cases, which give a different dependence of the distribution variance on T^2. In case the bell-shaped IMF the calculated ratio $\sqrt{\langle\alpha^2\rangle}/\langle\alpha\rangle$ varies somewhere between 0.02and 0.06. However, Fig. 4 shows that this ratio changes very little with the increase of the impurity concentration as well as with the variation of T in the case of measurements of all our samples. Obtained value of about 0.25 is much larger than that calculated above. Thus, we can conclude that the differences in the relative variance obtained by our measurements are not due to the distribution of internal IMF within the pore, but more likely due to differences in the distribution of pores in the different samples due to deviations in sample preparation, even though they were prepared according to the same procedure.

Fig. 6 shows that, in contrast to $\sqrt{\langle\alpha^2\rangle}/\langle\alpha\rangle$, the average of decay rate $\langle\alpha\rangle$ shows the dependence on both the impurity concentrations and on the frequency of spin phase modulation. The asymptotic transition of $\langle\alpha\rangle$ to the constant value at long T indicate that the measurements correspond to the long-time limit, which can be derived from Eq. (26) as

$$\langle\alpha(T)\rangle \approx \frac{1}{T_2} + \frac{4}{\pi^2}\left[\left(\langle\Delta\omega_1^2\rangle - \langle\Delta\omega_{01}\rangle\right)\frac{\tau_1 T^2}{T^2+\pi^2\tau_1^2} - \langle\Delta\omega_{11}\rangle\frac{T^2\tau_1/2}{T^2+\pi^2\tau_1^2/4}\right], \quad (27)$$

The calculation for the case of diffusion between parallel planes separated by d gives the decay rate dependence at long T for the IMF with a constant gradient, as well as for the IMF of cosine form [46], which both shows that in Eq. (27) $\langle\Delta\omega_1^2\rangle - \langle\Delta\omega_{01}\rangle = 0$ so that the characteristic time of the attenuation increase with $\tau_1/2$, where we assume where $\tau_1 \approx \frac{d^2}{\pi^2 D}$. In the case IMF with a bell shaped IMF, $\langle\omega_{in}\rangle \approx 12(x-d/2)^2/d^3$ [47], the predominant expression for the

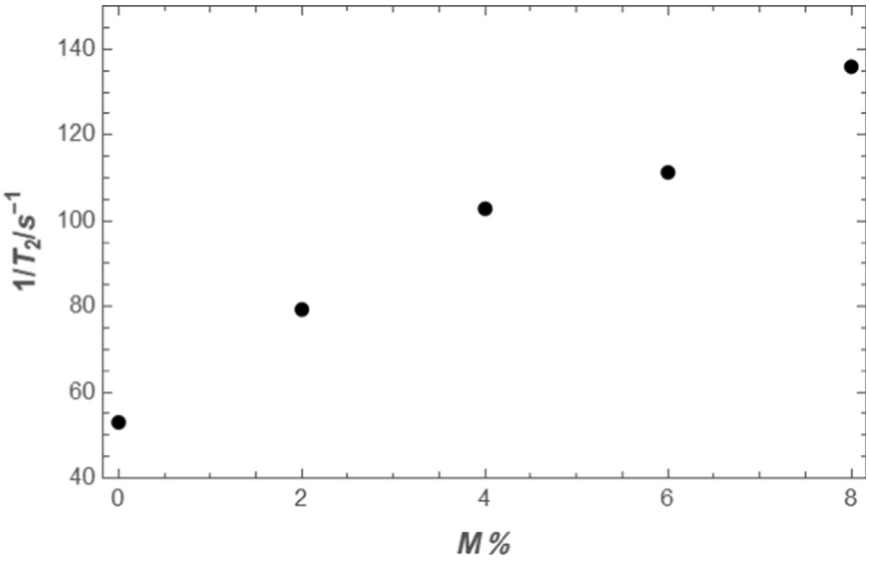

Fig. 7. Dependence of the spin relaxation rate on the content of magnetic impurities.

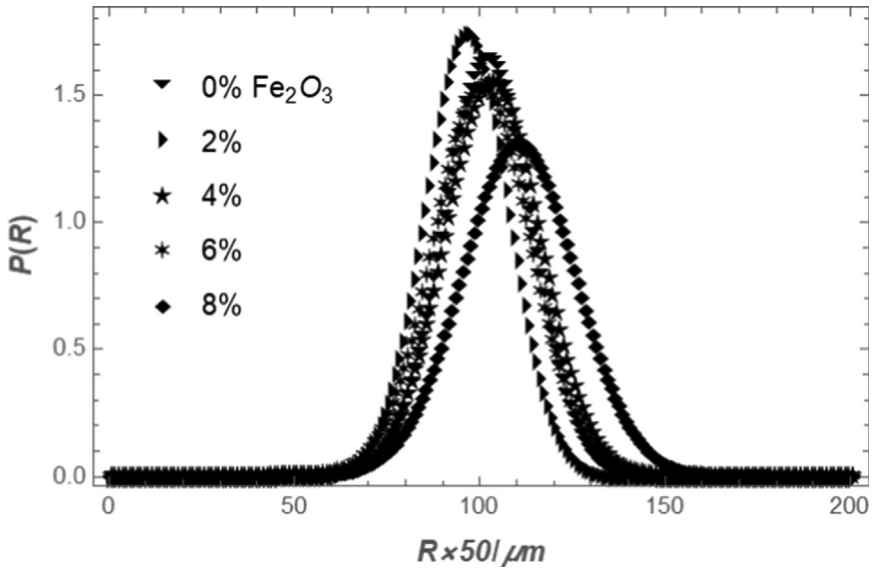

Fig. 8. The pore size distribution changes very little with the content of magnetic impurities.

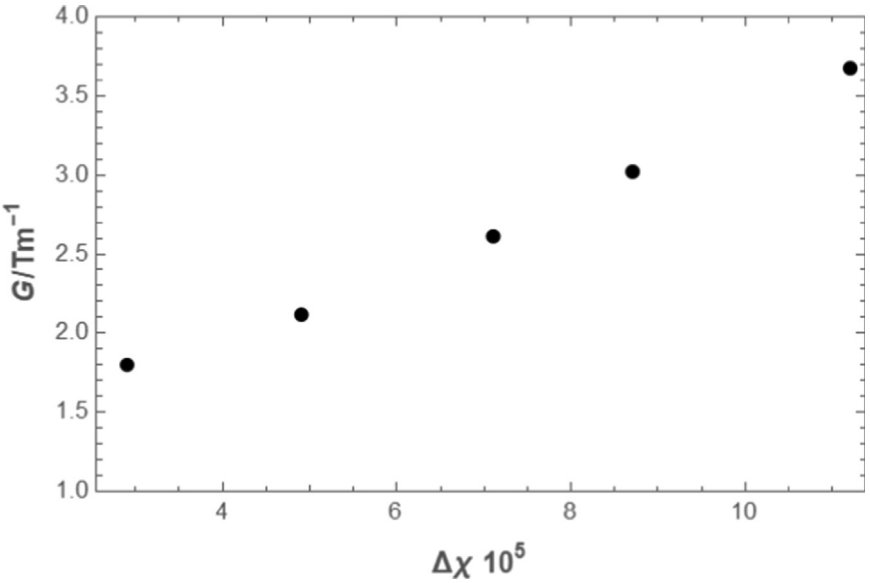

Fig. 9. The average internal gradient in ceramics as a function of the susceptibility difference measured by a vibrating magnetometer.

long T is $\langle \Delta\omega_{22} \rangle$ with characteristic time $\tau_1/8$, which means that the decay rate depends on the distribution of IMF within the pore volume.

Here we assume that the magnetic impurities generate a not too variable magnetic field within the pore volume which suggest the attenuation increases with a characteristic time that is about a half of the typical time of flight across the pore space, $\tau_1/2$, similar to the case with a homogeneous gradient or cosine-shaped IMF. The fitting of the second part of Eq. (27) with the experimental data shown in Fig. 6, we obtain from $\langle \alpha(T) \rangle$ the spin-relaxation $1/T_2$, the pore size and its distribution, and the internal IMF on the impurity concentrations. The dependence $1/T_2$ on the impurity concentration, shown in Fig. 7, cannot be explained by the effect of internal IMF [48,49] but more likely in the context of the impurity relaxation absorption (the slow relaxation mechanism) [50]. The pore size can be estimated from $\tau_1 = sR^2/D$, where R should be the pore radius, D is the diffusion coefficient, and s varies from 0.2314 for spherical pore, to 0.295 for cylindrical pore and to 0.405 for plan-parallel pore [44]. Since the pore geometry in ceramic is unknown, we assume a mean value $s \approx 0.3$, and the self-diffusion coefficient $D = 2.9 \cdot 10^{-9}$ m^2 s^{-1}, which is the mean value of the frequency dependent $D(\omega)$ in the interval $1 - 10$ kHz obtained by the MGSE measurements of water at 20 °C shown in reference [15]. Together with the obtained variances of the nonexponential decays $\sqrt{\langle \alpha^2 \rangle}/\langle \alpha \rangle$, it gives the dependence of the pore size and the normal distribution of pore size in ceramic on the content of magnetic impurities shown in Fig. 8. It shows that the average pore size roughly coincides with the values obtained from SEM measurements, where an estimated pore size was around 2–3 μm. One would expect that the appearance of large grains shown on Fig. 2 affects the distribution of internal magnetic fields. However, the rather mild dependence of attenuation variance $\langle \alpha^2 \rangle$ on T^2 shown in Fig. 4 compare to that shown in Fig. 5 does not confirm this. By the assumption that $\frac{4}{\pi^2}\langle \Delta\omega_{11} \rangle = \gamma^2 \langle G\, R \rangle^2$, the fitting

parameter $\langle \Delta\omega_{11} \rangle$ in Eq. (27) enables calculation of an average internal gradient. It is shown in Fig. 9 as a function of the susceptibility differences from Table 1, which were measured by a vibrating magnetometer.

In our experiments, the interval of the spin phase reversal, T, of the CPMG sequence does not exceed 1 ms, which means that the condition for the interpretation of experimental data according to Eq. (3) obtained using GPA theory would be met for MFG below 15 T/m in the case of water self-diffusion at room temperature. Given that in our case the observed average internal MFG in water-soaked ceramics does not exceed 4 T/m, GPA assumption is valid.

5. Conclusion

In the NMR studies of porous media, which are ubiquitous in modern life, from natural materials such as rocks, wood, and packed snow, to man-made materials such as concretes and food products, and to biologic tissues such as bones and lungs, the internally induced magnetic field created by the difference in magnetic susceptibility at interfaces in porous media and by magnetic impurities, are inevitable obstacle in the gradient spin echo measurements of the molecular self-diffusion as well as in the magnetic resonance imaging. The derived theory of spin dynamics under the influence of applied CPMG sequence and the IMF of different forms and strength can be used to interpret the measurements of ceramic samples doped with various concentration of magnetic impurities. The results of the experiments confirm the theory and prove its ability to provide relevant information on the porous structure, such as pore size and its distribution in porous medium, spin-relaxation time and average internal magnetic field at different contents of magnetic impurities.

Declaration of Competing Interest

The authors declare that they have no known competing financial interests or personal relationships that could have appeared to influence the work reported in this paper.

References

[1] I. Ardelean, R. Kimmich, Principles and unconventional aspects of nmr diffusometry, Annu. Rep. NMR Spectrosc. 49 (2003) 43–115.
[2] G.C. Borgia, R.J.S. Brown, P. Fantazzini, Scaling of spin-echo amplitudes with frequency, diffusion coefficient, pore size, and susceptibility difference for the nmr of fuids in porous media and biological tissues, Phys. Rev. E 51 (1995) 2104–2114.
[3] M.D. Hürlimann, Effective gradients in porous media due to susceptibility differences, J. Magn. Reson. 131 (1998) 232–240.
[4] B. Sun, K.-J. Dunn, Probing the internal field gradients of porous media, Phys. Rev. E 657 (2002) 51309.
[5] Y.Q. Song, Using internal magnetic fields to obtain pore size distributions of porous media, Magn. Reson. A 18 (2003) 97–110.
[6] H. Liu, M.N. d'Eurydice, S. Obruchkov, P. Galvosas, Determining pore length scales and pore surface relaxivity of rock cores by internal magnetic fields modulation at 2 mhz nmr, J. Magn. Reson. 246 (2014) 110–118.
[7] L.J. Zielinski, Effect of internal gradients in the nuclear magnetic resonance measurement of the surface-to-volume ratio, J. Chem. Phys. 121 (2004) 352–361.
[8] J.G. Seland, K.E. Washburn, H.W. Anthonsen, J. Krane, Correlations between diffusion, internal magnetic field gradients, and transverse relaxation in porous systems containing oil and water, Phys. Rev. E 70 (2004) 051305.
[9] S. Muncaci, C. Mattea, S. Stapf, I. Ardelean, Frequency-dependent nmr relaxation of liquids confined inside porous media containing an increased amount of magnetic impurities, Magn. Reson. Chem. 51 (2013) 123–128.
[10] H. Cho, S. Ryu, J. Ackerman, Y.-Q. Song, Visualization of inhomogeneous local magnetic field gradient due to susceptibility contrast, J. Magn. Reson. 198 (2009) 88–93.
[11] S. Puwa, B.J. Roth, P.J. Basser, Heterogeneous anisotropic magnetic susceptibility of the myelin-water layers causes local magnetic field perturbations in axons, NMR Biomed. (2016), https://doi.org/10.1002/andp.19063261405.
[12] X. Liu, C. Chen, T. Qu, K. Yang, H. Luo, Transverse spin relaxation and diffusion-constant measurements of spin-polarized 129xe nuclei in the presence of a magnetic field gradient, Sci. Rep. 6 (2016) 24122.
[13] J. Stepišnik, I. Ardelean, Usage of internal magnetic fields to study the early hydration process of cement paste by mgse method, J. Magn. Reson. 272 (2016) 100–107.
[14] J. Stepišnik, P. Callaghan, The long time-tail of molecular velocity correlation in a confined fluid: observation by modulated gradient spin echo nmr, Phys. B 292 (2000) 296–301.
[15] J. Stepišnik, C. Mattea, S. Stapf, A. Mohorič, Molecular velocity auto-correlation of simple liquids observed by nmr mgse method, Eur. Phys. J. B 91 (2018) 293, https://doi.org/10.1140/epjb/e2018-90284-4.
[16] A. Mohorič, J. Stepišnik, Nmr in the earth's magnetic field, Prog. Nucl. Magn. Reson. Spectrosc. 54 (2009) 166–182.
[17] N. van Kampen, Stochastic Processes in Physics and Chemistry, North-Holland Publishing Company, Amsterdam, 1981.
[18] E.O. Stejskal, Use of spin echoes in a pulsed magnetic field gradient to study anisotropic, restricted diffusion and flow, J. Chem. Phys. 43 (1965) 3597–3603.
[19] H.C. Torrey, Bloch equations with diffusion terms, Phys. Rev. 104 (1956) 563–565.
[20] J. Kärger, W. Heink, The propagator representatin of molecular transport in microporous crystallites, J. Magn. Reson. 51 (1983) 1–7.
[21] P.T. Callaghan, D. MacGowan, K.J. Packer, F.O. Zelaya, High resolution q-space imaging in porous structures, J. Magn. Reson. 90 (1990) 177–182.
[22] R. Kubo, Some Aspects of the Statistical-Mechanical Theory of Irreversible Processes, Lectures on Theoretical Physics, Interscience Publisher, 1959.
[23] M.D. Hürlimann, L.M. Schwartz, P. Sen, Probability of returns to the origin at short times: A probe of microstructure in porous media, Phys. Rev. B 51 (1995) 14936–14940.
[24] A.L. Bratland, T. Pavlin, K. Djurhuus, J.G. Seland, Characterising oil and water in porous media using correlations between internal magnetic gradient and transverse relaxation time, J. Mag. Res. 310 (2020) 106649.
[25] J. Stepišnik, Averaged propagator of restricted motion from the gaussian approximation of spin echo, Phys. B 344 (2004) 214–223.
[26] J. Stepišnik, Analysis of nmr self-diffusion measurements by density matrix calculation, Phys. B 104 (1981) 350–364.
[27] P. Callaghan, J. Stepišnik, Advances in Magnetic and Optical Resonance, ed. Warren S. Warren, volume 19, Academic Press Inc, San Diego, 1996, pp. 326–89.
[28] J. Stepišnik, C. Mattea, S. Stapf, A. Mohorič, Molecular velocity auto-correlations in glycerol/water mixtures studied by nmr mgse method, Phys. A 553 (2020) 124171, https://doi.org/10.1016/j.physa.2020.124171.
[29] A.Y. Khinchin, Korrelationstheorie der stationären stochastischen prozesse, Math. Ann. 109 (1934) 604–615.
[30] J. Stepišnik, S. Lasič, A. Mohorič, I. Serša, A. Sepe, Velocity autocorrelation spectra of fluid in porous media measured by the cpmg sequence and constant magnetic field gradient, Magn. Reson. Imaging 25 (2007) 517–520.
[31] H.Y. Carr, E.M. Purcell, Effects of diffusion on free precession in nuclear magnetic resonance, Phys. Rev. 94 (1954) 630–638.
[32] S. Meiboom, D. Gill, Modified spin-echo method for measuring nuclear relaxation times, Rev. Sci. Inst. 29 (1958) 688–691.
[33] P. Callaghan, J. Stepišnik, Frequency-domain analysis of spin motion using modulated gradient nmr, J. Magn. Reson. A 117 (1995) 118–122.
[34] P.T. Callaghan, S.L. Codd, Flow coherence in a bead pack observed using frequency domain modulated gradient nuclear magnetic resonance, Phys. Fluids 13 (2001) 421–426.
[35] D. Topgaard, C. Malmborg, O. Soederman, Restricted self-diffusion of water in a highly concentrated w/o emulsion studied using modulated gradient spin-echo nmr, J. Mag. Res. 156 (2002) 195–201.
[36] E.C. Parsons, M.D. Does, J.C. Gore, Modified oscillating gradient pulses for direct sampling of the diffusion spectrum suitable for imaging sequences, Magn. Reson. Imaging 21 (2003) 279–285.
[37] D.T.S. Lasič, I. Aslund, Spectral characterization of diffusion with chemical shift resolution: Highly concentrated water-in-oil emulsion, J. Mag. Res. 199 (2009) 166–172.
[38] J.G. Seland, High frequency modulated gradient spin echo diffusion measurements with chemical shift resolution, diffusion-fundamentals.org 7 (2010) 1–4.
[39] J. Stepišnik, S. Lasič, A. Mohorič, I. Serša, A. Sepe, Spectral characterization of diffusion in porous media by the modulated gradient spin echo with cpmg sequence, J. Mag. Res. 182 (2006) 195–199.
[40] S. Lasič, J. Stepišnik, A. Mohorič, I. Serša, G. Planinšič, Autocorrelation spectra of an air-fluidized granular system measured by nmr, Europhys. Lett. 75 (2006) 887–893.
[41] J.F. Kenney, E.S. Keeping, Cumulants and the Cumulant-Generating Function, Van Nostrand, New York, 1951.
[42] P. Stilbs, Fourier transform pulsed-gradient spin-echo studies of molecular diffusion, Prog. NMR Spectrosc. 19 (1987) 1–45.
[43] E. Oppenheim, P. Mazur, Brownian motion in system of finite size, Physica 30 (1964) 1833–1845.
[44] J. Stepišnik, Time dependent self-diffusion by nmr spin-echo, Phys. B 183 (1993) 343–350.
[45] S. Stapf, R. Kimmich, Molecular dynamics in confined monomolecular layers. a field-cycling nuclear magnetic resonance relaxometry study of liquids in porous glass, J. Chem. Phys. 103 (1995) 2247–2250.

[46] D.S. Grebenkov, Nuclear magnetic resonance restricted diffusion between parallel planes in a cosine magnetic field: An exactly solvable model, J. Chem. Phys. 126 (2007) 104706.
[47] W.S. Price, NMR Studies of Translational Motion, Cambridge Molecular Science, Cambridge, New York, Melbourne, Madrid, Cape Town, Singapore, Sao Paulo, Delhi, 2009.
[48] K.-J. Dunn, Enhanced transverse relaxation in porous media due to internal field gradients, J. Magn. Reson. 156 (2002) 171–180.
[49] L.J. Zielinski, P. Sen, Relaxation of nuclear magnetization in a nonuniform magnetic field gradient and in a restricted geometry, J. Magn. Reson. 147 (2000) 95–103.
[50] A.V. Zalesskii, V.G. Krivenko, V.S. Lutovinov, T. Khimich, V.N. Shadonov, K. Tompa, P. Banky, Effect of paramagnetic impurity on spin-spin and spin-lattice relaxation of ^{57}Fe nuclei in hematite, Zh. Eksp. Teor. Fiz. 86 (1984) 1891–1899.